# Relationships between DNA strand breakage and apoptotic progression upon treatment of HL-60 leukemia cells with tafluposide or etoposide

Jérôme Kluza[a], Romain Mazinghien[a], Helen Irwin[b], John A Hartley[b] and Christian Bailly[c]

**Tafluposide (F11782), an epipodophyllotoxin derivative currently undergoing phase I clinical trials, is structurally close to the established anti-cancer drug etoposide, but mechanistically distinct. It is a dual inhibitor of topoisomerases I and II which impairs the binding of the enzyme to DNA, but does not stabilize the cleavage complex. Nevertheless, both etoposide and tafluposide induce DNA strand breaks and are potent pro-apoptotic agents. In this study, we have compared the cellular response of HL-60 human promyelocytic leukemia cells treated with etoposide and tafluposide. We show that tafluposide induces delayed, but extensive, DNA strand breaks, whereas etoposide provokes rapid and massive DNA damage. The two drugs trigger similar types of alterations at the mitochondrial and cell cycle levels, and lead to the generation of comparable levels of reactive oxygen species, but with different kinetics. Our data suggest that modification of the mitochondrial mass plays an important role in apoptosis induced by DNA-damaging anti-cancer agents, at least in the epipodophyllotoxin series. We suggest that drug-induced mitochondrial alterations can be divided into three successive steps: (i) hyperpolarization, (ii) depolarization and (iii) increase of the mitochondrial mass.** *Anti-Cancer Drugs* **17:155–164**


**Anti-Cancer Drugs** 2006, **17**:155–164

**Keywords: apoptosis, Comet assay, DNA strand break, etoposide, mitochondria, reactive oxygen species, tafluposide, topoisomerase**

[a]INSERM U524, Institut de Recherche sur le Cancer de Lille, Lille, France, [b]Cancer Research UK Drug–DNA Interactions Research Group, Department of Oncology, UCL, London, UK and [c]Institut de Recherche Pierre Fabre, Toulouse, France.

Correspondence to C. Bailly, Centre de Recherche en Oncologie Expérimentale, Institut de Recherche Pierre Fabre, 3 rue des satellites, 31400 Toulouse, France. Tel: +33 534 32 14 44; fax: +33 534 32 14 34; e-mail: christian.bailly@pierre-fabre.com

**Received** 25 September 2005 **Accepted** 29 September 2005

## Introduction

Tafluposide (Fig. 1) is a dual inhibitor of topoisomerases I and II with a novel mechanism of action [1–6]. Inhibition of topoisomerase II is principally responsible for its cytotoxic effects [7]. This hemisynthetic epipodophyllotoxin derivative impairs the binding of topoisomerase enzymes to DNA, but, unlike its structurally close analog etoposide (Fig. 1), it does not stabilize covalent DNA–enzyme phosphotyrosyl complexes [8]. Like etoposide, it shows no affinity for DNA and likely interferes directly with the enzyme to prevent proper enzyme–DNA interaction. Binding of epipodophyllotoxins to topoisomerase II has been well documented for etoposide [9,10]. Tafluposide and etoposide thus share the same target, but they affect its functioning in a distinct manner. The differences in terms of recognition and blockade of the target suggest that the extent, nature and/or kinetics of cellular DNA damage induced by the two compounds may also be different, and this is the issue we addressed in this study.

Tafluposide is a potent inhibitor of nucleotide excision repair, acting during the incision step [5,7]. *In vivo*, the anti-tumor activity of tafluposide is markedly superior to that of other catalytic topoisomerase inhibitors and the compound is currently undergoing phase I clinical trials [11–14]. Tafluposide is also a potent pro-apoptotic agent. In the P388 murine leukemia cell line, the drug induces caspases activation, poly(ADP-ribose) polymerase cleavage and an increase of the Bax/Bcl-2 ratio. It has been suggested that the 'mitochondrial pathway' is implicated in tafluposide-induced apoptosis, but so far this hypothesis had not been precisely addressed [15]. Accordingly, here we have compared the extent and kinetics of apoptosis induced by tafluposide versus etoposide using HL-60 human promyelocytic cells. A time-course investigation of the drug-induced mitochondrial and nuclear alterations is reported. The discussion centers around the increase of the mitochondrial mass induced by the two drugs and the general implication of this process for DNA-damaging agents.

## Materials and methods

### Drug and chemicals

Tafluposide (F11782) was provided from the Pierre Fabre Laboratories (Toulouse, France). The drug was dissolved in DMSO to obtain a 25 mmol/l stock solution and in all cases fresh working solutions were prepared extemporaneously. RNase A and propidium iodide (PI) were purchased from Sigma (St Louis, Missouri, USA).

0959-4973 

**Fig. 1**

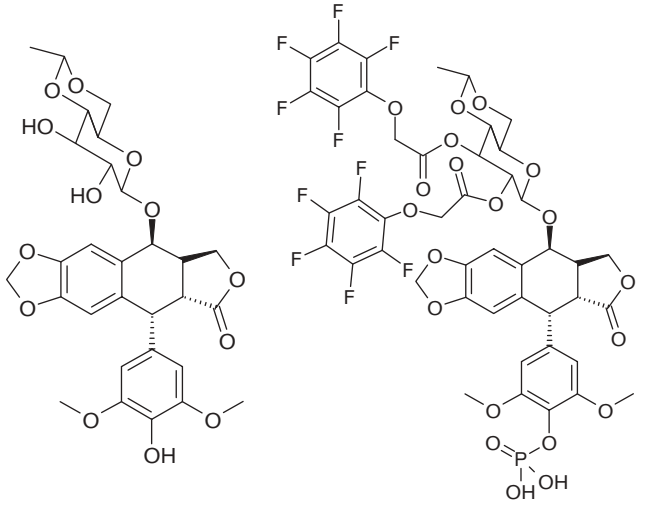


Structures of etoposide and tafluposide (F11782: 2″,3″-bis pentafluorophenoxy-acetyl-4″,6″-ethylidene-β-D-glucoside of 4′-phosphate-4′-demethylepipodophyllotoxin, 2*N*-methyl glucamine salt).

5,5′,6,6′-Tetrachloro-1,1′,3,3′-tetraethylbenzimidazolcarbocyanine (JC-1), 3,8-phenanthridinediamine, 5-ethyl-5,6–dihydro–6-phenyl [hydroethidine (HE)], mitotracker green (MTG) and 4′-6-diamidino-2-phenylindole dihydrochloride (DAPI) were obtained from Molecular Probes (Eugene, Oregon, USA).

### Cells and culture conditions

The HL-60 leukemia cell line was obtained from the ATCC (Manassas, Virginia, USA; CCL 240). Cells were grown at 37°C under 5% $CO_2$/air in RPMI medium containing 100 U/ml penicillin/0.1 ng/ml streptomycin and supplemented with 10% heat-inactivated FCS. Prior to the drug treatment, exponentially growing cells ($25 \times 10^4$ in 1 ml) were seeded in 24-well plates for 2 h prior to the incubation with the drug. Drug concentrations and exposure times are indicated in the figure legends.

### Cell cycle variations and nuclear apoptosis

Hypoploid (sub-$G_1$) cells were characterized by cell cycle measurements. Cells were fixed overnight at 4°C in 70% ice-cold ethanol/PBS and then stained with a solution containing PI (50 μg/ml) and RNase A (0.5 mg/ml), and analyzed with a Becton Dickinson FACScan cytofluorometer. Data were analyzed with WinMDI software.

### Nucleus and cytoplasm morphology

Chromatin condensation was assessed by staining cells with DAPI (2.5 mg/ml) after fixation of cells in 70% cold ethanol for 4 h at −20°C and then the nuclear morphology was visualized by fluorescence microscopy using a Zeiss microscope with a × 63 or × 100 oil objective. Images were captured using the software Quips Smart Capture (Vysis). For the morphological assessment of apoptosis by light microscopy, cells were stained with the standard Papanicolaou procedure.

### Cytofluorometric analysis of mitochondrial changes

To evaluate the mitochondrial transmembrane potential ($\Delta\psi_m$), a procedure described previously was followed [16]. Briefly, cells ($5 \times 10^5$/ml) were incubated for 30 min at 37°C with the fluorescent probe JC-1 (1 μmol/l in PBS). Samples were stored on ice prior to the cytofluorometric analysis. JC-1 exists as a monomer at low values of $\Delta\psi_m$ (green fluorescence; emission at 527 nm), while it forms aggregates at high $\Delta\psi_m$ (orange fluorescence; emission at 590 nm). Changes in the mitochondrial mass were analyzed with the mitochondrion-specific dye MTG. This fluorochrome preferentially accumulates in mitochondria. MTG (100 nmol/l) was added to the cell suspension ($5 \times 10^5$/ml) and incubated for 30 min at 37°C. Monoparametric analysis was performed on the FL1 channel and the mean fluorescence intensity (MFI) was measured. It is worth noting here that binding of MTG to the mitochondrial membrane can be affected when mitochondria are de-energized. However, this effect generally occurs at a high concentration of MTG. We have adapted our experimental conditions to ascertain that in the present case the variations of the fluorescence of MTG reflect changes of the mitochondrial mass, independently of the potential variations of $\Delta\psi_m$.

### Cytofluorometric analysis of reactive oxygen species (ROS)

The production of peroxides was determined using the non-fluorescent substance HE which is oxidized by hydroxyl radicals to give a product emitting a red fluorescence. Cells ($25 \times 10^4$/ml) were exposed for 30 min at 37°C to 2.5 μmol/l HE prior to the cytofluorometric analysis (excitation 355 nm; emission 420 nm).

### Comet assay

Cells ($1.25 \times 10^4$ in 0.5 ml ice-cold PBS) were mixed with 0.9 ml 1% low-gelling temperature agarose (Sigma; type VII). The mixture was rapidly put onto microscope precoated slides (1% agarose) on ice. Slides were immediately incubated in 500 ml of lysis buffer (100 mmol/l EDTA, 2.5 M sodium chloride, 10 mmol/l Tris–HCl, pH adjusted to 10.5 with sodium hydroxide pellets and 1% Triton X-100 to be added immediately before use in the assay) for 1 h at 4°C in the dark. Slides were washed with distilled water 4 times during 1 h and then incubated for 45 min with alkali electrophoresis buffer (50 mmol/l sodium hydroxide, 1 mmol/l disodium EDTA, pH 12.5). Electrophoresis was performed at 18 V (0.6 V/cm)/250 mA for 25 min in the dark. Slides were washed successively with neutralization buffer (0.5 M Tris–HCl, pH 7.5) and PBS, pH 7.4. Slides were dried

overnight at room temperature, rehydrated the next day with distilled water for 45 min and finally stained with a PI solution (2.5 μg/ml for 20 min), washed with distilled water, and dried in an oven for 2 h. Slides were analyzed with a Zeiss epifluorescence microscope. Comet images were measured using Komet software (Kinetic Imaging, Nottingham, UK) and the amount of strand break damage quantitated as Olive tail moment (% DNA in tail × distance between the means of head and tail distributions).

## Results

HL-60 cells were treated with increasing concentrations of etoposide or tafluposide for 24 h prior to PI staining and analysis with a flow cytometer (Fig. 2a). Low etoposide concentrations (from 0.1 to 1 μmol/l) provoked an accumulation of cells in the $G_2$/M phase. At a higher concentration (5 μmol/l), a shift toward the $G_1$/S phase was observed followed by a characteristic hypoploid DNA content peak (sub-$G_1$ cells represent 45% after 24 h). The cell cycle profiles of tafluposide-treated cells show similar changes. From 0.1 to 10 μmol/l, cells were arrested in the $G_2$/M phase; however, treatment with a higher concentration induced a significant accumulation in the S phase with a few sub-$G_1$ cells. At 50 μmol/l, the fraction of sub-$G_1$ cells only represented 11% of the cell population. Concentrations above 50 μmol/l were not tested due to the appearance of tafluposide-induced necrosis (as seen by Trypan blue exclusion, data not shown). This first set of cell cycle data suggests that there is a difference between tafluposide and etoposide in terms of nuclear apoptosis after 24 h of drug treatment. This issue was investigated further using the drug concentrations required for the appearance of significant nuclear alterations: 50 μmol/l for tafluposide and 5 μmol/l etoposide. The ratio of 10 reflects the different cytotoxic potential of the compounds. In an MTT assay, $IC_{50}$ values of 1.3 and 0.11 μmol/l were calculated for tafluposide and etoposide, respectively.

To confirm the induction of apoptosis, drug-treated HL-60 cells were stained with the fluorescent DNA-binding drug DAPI (Fig. 2b) or according to the Papanicolaou procedure (Fig. 2c). Considerable perturbations of the nuclear and cellular morphology were seen by microscopy in the presence of etoposide, but not with tafluposide. Tafluposide-treated cells (50 μmol/l) do not show any critical modification when compared with untreated cells. Nuclei are slightly bigger and a few apoptotic bodies, with cytoplasm and chromatin condensation, were detected (below 10%). In contrast, etoposide-treated cells (5 μmol/l) appeared much smaller than untreated cells, with a condensed cytoplasm and a fragmented nucleus. In these microscopy experiments, the proportion of apoptotic cells was comparable with that seen in the cell cycle experiments (40–50%).

Next, time-course experiments with tafluposide (50 μmol/l) and etoposide (5 μmol/l) were performed to measure the capacity of the drug to induce nuclear apoptosis after 1–4 days of treatment. As above, cells were stained with PI and analyzed by flow cytometry (Fig. 3a). The percentage of sub-$G_1$ cells in etoposide-treated cells increased proportionally during the period of incubation and concomitantly $G_1$/S arrested cells decreased. About 64% of sub-$G_1$ cells were detected after 48 h of drug treatment, and this percentage remained roughly equivalent at 72 and 96 h (Fig. 3b). Surprisingly, sub-$G_1$ cells were detected with tafluposide after 24 h of treatment. At 48 h, most of the cells were arrested in the S phase, but the apoptotic cell fraction was increased to reach 37% after 4 days of treatment with tafluposide. These experiments show that both tafluposide and etoposide are able to induce nuclear apoptosis in HL-60 cells, but the kinetics are different (Fig. 3b).

Mitochondrial changes are often described during drug-induced apoptosis. Usually, these perturbations precede nuclear apoptosis and are the key events of the process. These considerations prompted us to analyze the mitochondrial function, including $\Psi_m$ and mitochondrial mass. To evaluate the mitochondrial alterations during drug treatment (Fig. 4), we measured $\Delta\Psi_m$ by cytometry using the fluorescent probe JC-1, which is considered as one of the most mitochondria-specific probe [17]. Mitochondria with normal $\Delta\Psi_m$ concentrate JC-1 into aggregates (orange fluorescence), while in depolarized mitochondria JC-1 aggregates are dissociated in JC-1 monomers (green fluorescence). After 4 h of cell treatment with etoposide, the JC-1 profiles were modified. Cells shifted simultaneously from higher orange fluorescence and lower green fluorescence, indicating hyperpolarization of the mitochondria. These data confirm our previously published results with etoposide [18]. After 9 h of treatment, a decrease of JC-1 aggregates was observed and this is a characteristic of mitochondria depolarization. At 14 h, the green fluorescence increased considerably – an effect we could show recently to reflect an increase of the mitochondrial mass [16]. Similar mitochondrial membrane modifications were shown in tafluposide-treated cells, but a delay was observed. Typical changes characterizing the mitochondrial hyperpolarization occurred after 14 h of treatment, the mitochondrial depolarization was noticed after 24 h and, finally, a mitochondrial mass increase appeared at 48 h.

In general, the JC-1 probe is used to measure the $\Delta\Psi_m$, but not the variations of the mitochondrial mass. For this reason, to consolidate our observations, we have confirmed our results with the probe MTG which is known as a specific marker of the mitochondrial mass [19]. Accumulation of MTG in mitochondria is independent of $\Psi_m$. Cells were treated with each drug, stained with MTG, and the MFI measured by flow cytometry and

**Fig. 2**

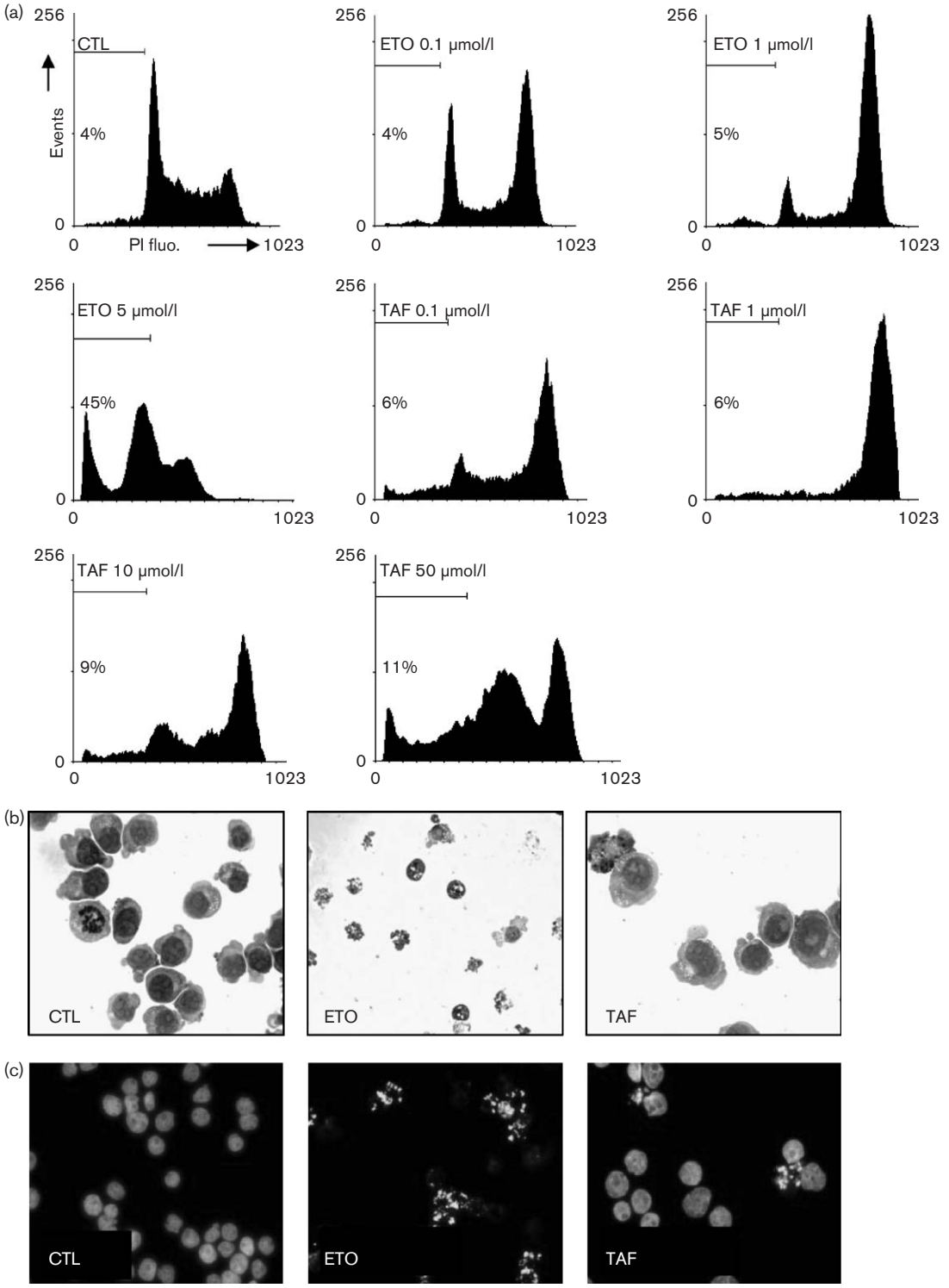


Apoptotic features of HL-60 treated with tafluposide or etoposide. Cells were incubated for 24 h with the test drugs. (a) Cell cycle effects and apoptosis were determined by flow cytometry, at the indicated drug concentration. The percentage of sub-$G_1$ cells (hypoploid population) is indicated on each panel. Results are representative of three independent experiments. Morphological changes in HL-60 cells treated with 5 µmol/l etoposide and 50 µmol/l tafluposide were analyzed under the microscope by Papanicolaou staining (b), and nuclear condensation/fragmentation was detected by DAPI staining of nuclei (c), original magnification × 400.

**Fig. 3**

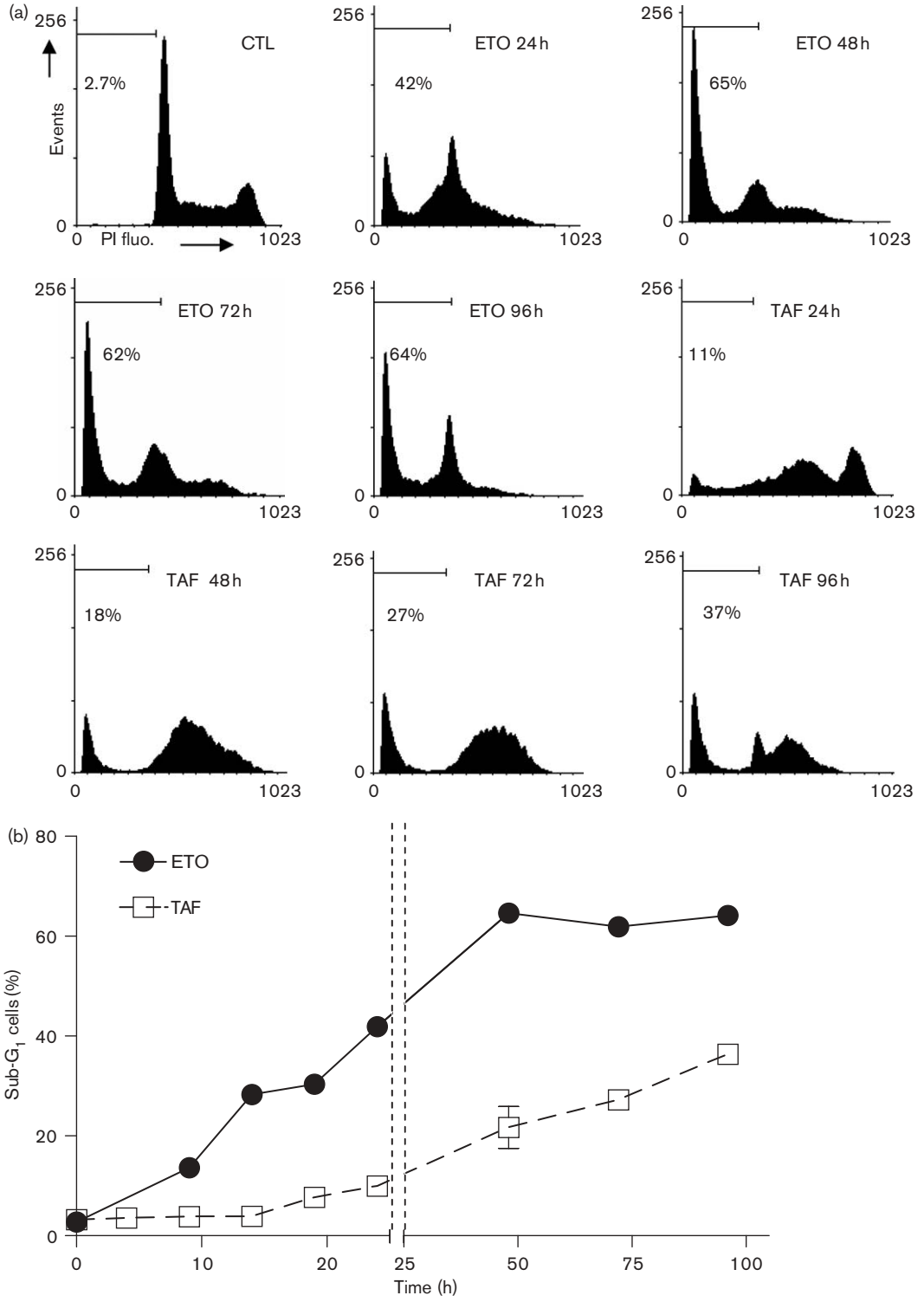


Time course of nuclear apoptosis induction in HL-60 cells. (a) Cells were treated with 5 μmol/l etoposide or 50 μmol/l tafluposide for 24, 48, 72 and 96 h. Cell cycle variations and apoptosis were determined by flow cytometry as in Fig. 2. (b) Quantification (%) of the time-dependent appearance of sub-$G_1$ cells upon treatment with etoposide and tafluposide.

**Fig. 4**

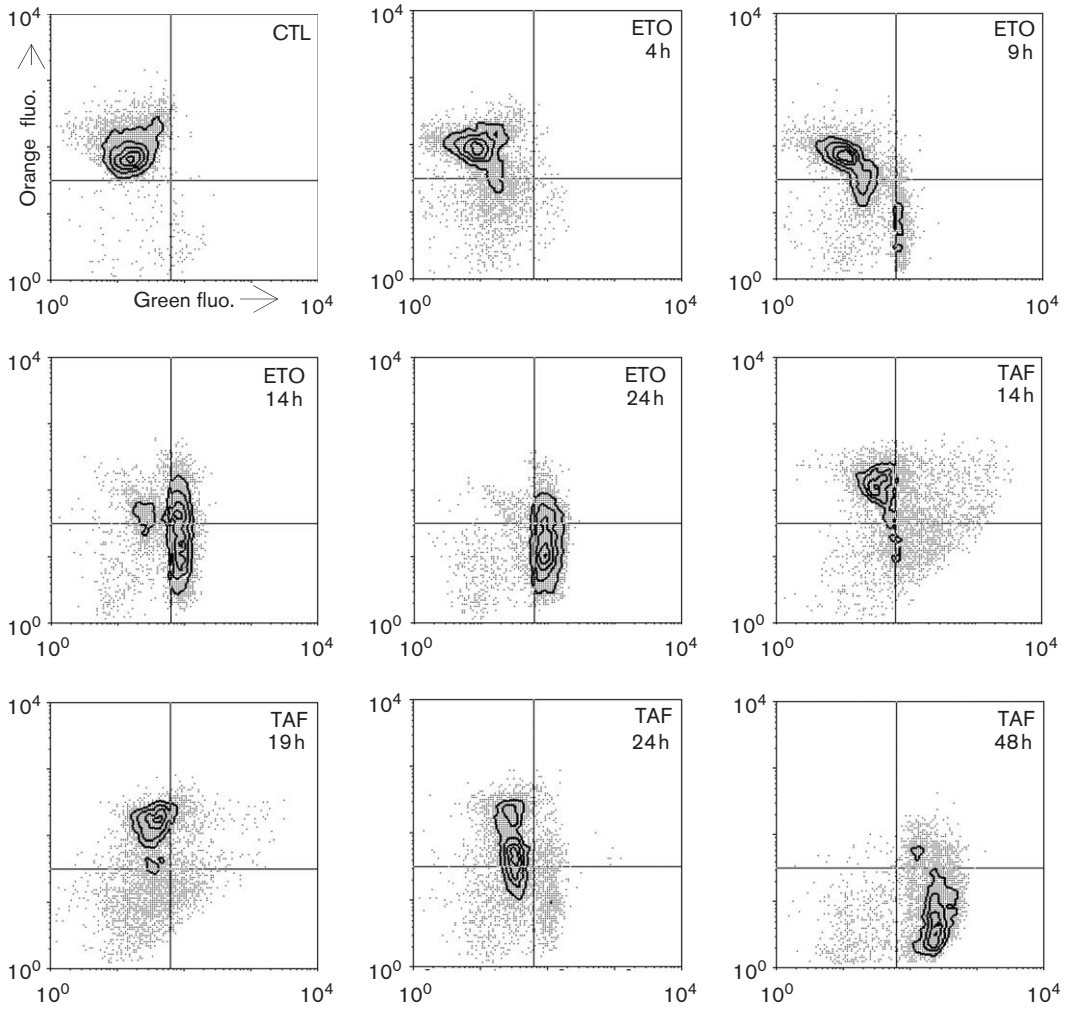


Variations of $\Delta\Psi_m$ in drug-treated HL-60 cells. Cytofluorometric analysis of JC-1 fluorescence in HL-60 cells treated with etoposide (5 μmol/l) and tafluposide (50 μmol/l) during the indicated times. Data represent typical results of one out of three independent experiments.

compared to that measured in untreated control cells (Fig. 5a). From 4 h of treatment with etoposide, the MTG fluorescence increased only slightly compared to untreated cells, but from 14 h a much larger increase was observed and was roughly stabilized after 24–30 h. These data are reminiscent to those obtained with the JC-1 probe, as shown above. Interestingly, the kinetics of the MTG fluorescence variation was significantly distinct with tafluposide (Fig. 5a). In this case, the MTG fluorescence increased from 48 h and continued up to 72 h. These experiments demonstrate that the sequence of mitochondrial alterations is identical for the two drugs – the first alteration is an early hyperpolarization of mitochondrial membranes, followed by a depolarization phase and then a mitochondrial mass increase. However, the time of appearance of the changes is delayed in response to tafluposide, as compared to etoposide.

In a previous paper, we have suggested a link between the production of ROS and the variation of the mitochondrial mass during apoptosis induced by doxorubicin (which is also a topoisomerase II inhibitor) in mammary adenocarcinoma MTLn3 tumor cells [16]. For this reason, by analogy, we went on evaluating the oxidative stress in drug-treated HL-60 using the probe HE, which is converted into a red fluorescent dye (ethidium) after oxidation by ROS. As shown in Fig. 5(b), the early phase of ROS production could be measured in HL-60 cells after 9 h of treatment with etoposide, whereas it took up to 24 h to observe a similar effect with tafluposide. The results suggest that ROS production precedes mitochondrial mass increase and accompanies mitochondria depolarization.

All the above data confirmed that etoposide and tafluposide induce apoptosis by similar pathways, involving

**Fig. 5**

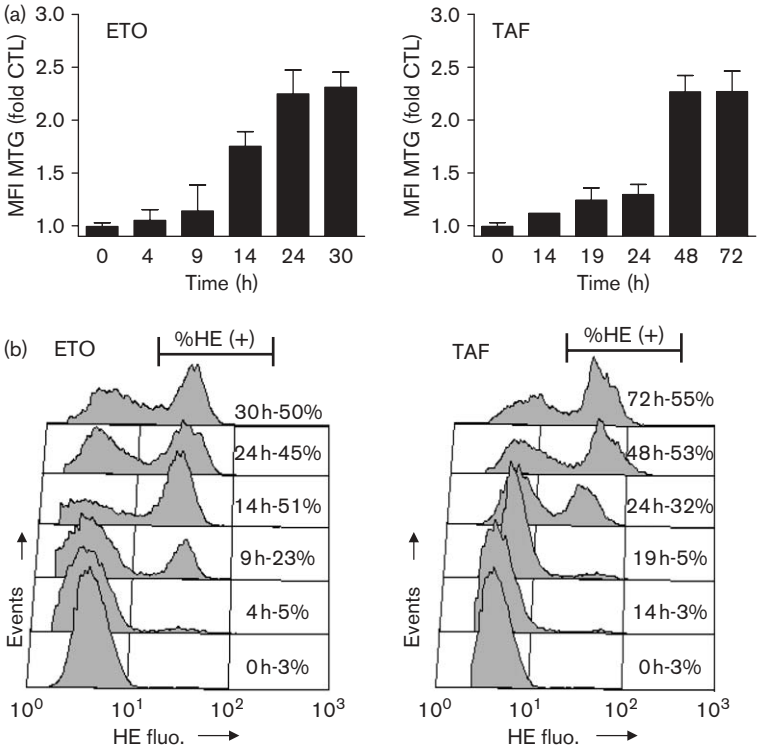


Kinetics of variations of the mitochondrial mass and ROS production upon drug treatment. Cells were cultivated in the presence of etoposide (5 μmol/l) and tafluposide (50 μmol/l) for the indicated time. (a) The mitochondrial mass was measured by flow cytometry using the MTG fluorescent dye. The relative MFI (MFI ± SEM of three independent experiments) was determined. (b) ROS production. Cells were treated with the drug at the indicated time and then labeled with HE which emits red fluorescence upon oxidation by ROS. The percentage of ROS-producing cells emitting high red fluorescence was measured by flow cytometry [HE (+)].

mitochondrial and nuclear alterations. The only significant difference was seen at the kinetics level, with an important delay observed with tafluposide. It is interesting to establish a link between these observations and those of Barret *et al.* [6], who showed that etoposide and tafluposide induced different levels and kinetics of DNA strand break in CHO-K1 cancer cells. On this basis, we hypothesized that the kinetics of DNA strand breaks induced by tafluposide and etoposide in HL-60 cells could explain the difference in terms of mitochondrial apoptosis. To study this hypothesis, we performed a time-course analysis of DNA strand breaks in HL-60 treated with tafluposide and etoposide using the Comet assay, and the amount DNA strand breakage was quantified by the increase of the tail moment (Fig. 6a and b).

The appearance of 'comets' characterizing DNA damage took place after 1 h of treatment with etoposide (Fig. 6a) and the level of DNA damage increased with time. In fact, etoposide induced an early increase in the tail moment, which reached a plateau after 2 h of treatment (Fig. 6b). In comparison, treatment with tafluposide induced much fewer DNA strand breaks from 1 to 4 h (Fig. 6a and b). DNA strand breaks appeared later, increasing almost linearly for the first 8 h, and then reached the level seen with etoposide (Fig. 6b). These results fully agreed with the microscopy observations (Fig. 2a and c).

## Discussion

Etoposide and tafluposide are two structurally related epipodophylloid (Fig. 1) anti-tumor agents targeting topoisomerase II, and showing potent activities *in vivo* against a number of human tumor models [20]. The incorporation of the two pentafluorophenol groups on the carbohydrate moiety of etoposide has modified the reactivity of tafluposide toward the enzyme. This structural change converts the poison etoposide into a catalytic inhibitor and this mechanistic modification translates into a different spectrum of anti-tumor activity [7,11,14]. Tafluposide exhibits synergistic effects when combined with cisplatin in ovarian cancer cells and with etoposide in acute myeloid leukemia [21]. This compound developed by the Pierre Fabre Laboratories showed highly potent anti-tumor effects *in vivo* in various

**Fig. 6**

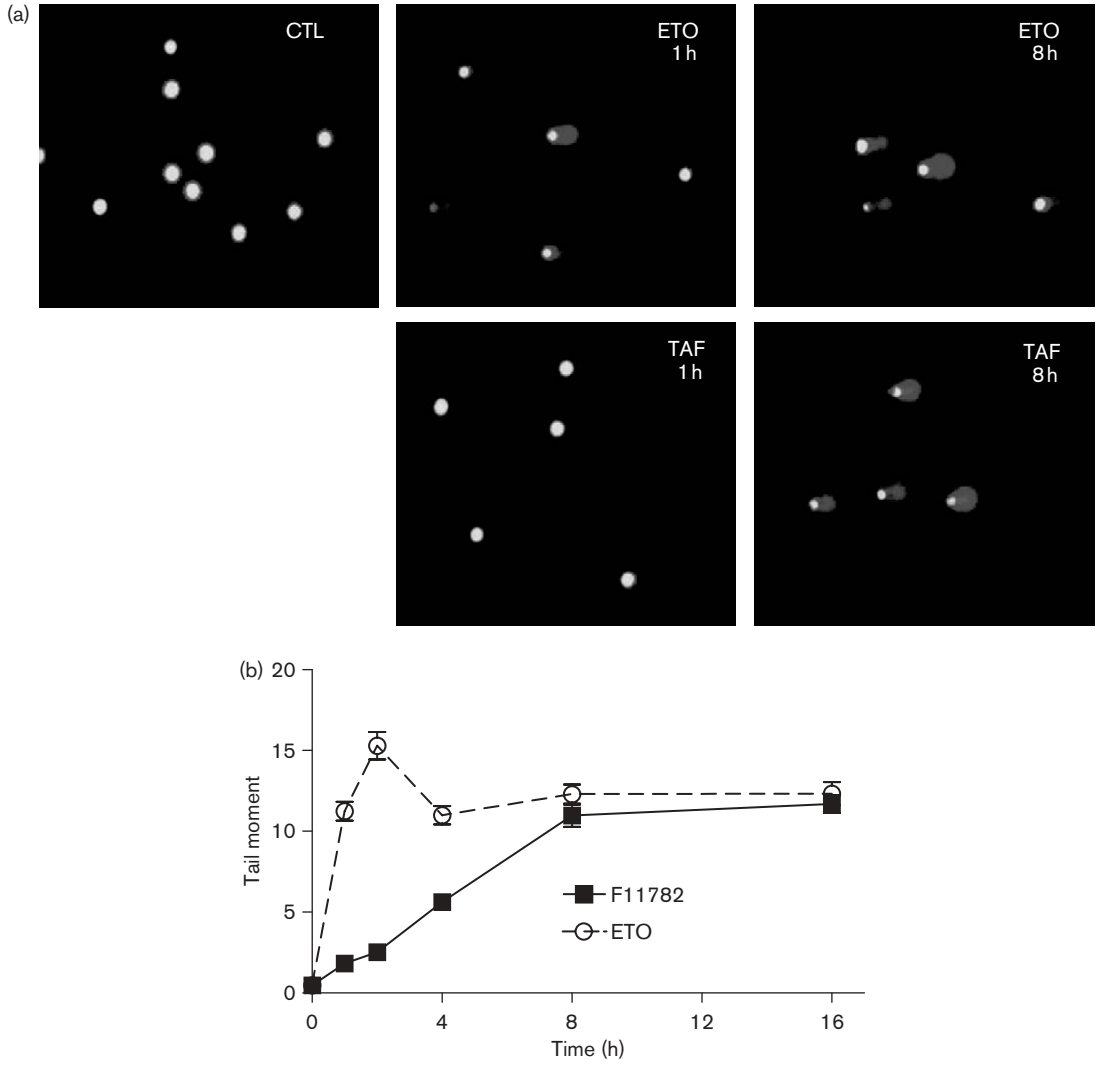


Time course of DNA damage evaluated by the Comet assay. Cells were treated with etoposide (5 μmol/l) and tafluposide (50 μmol/l) for the indicated times. (a) Each photomicrograph (× 400) is a representative view of a full slide. (b) Variation of the tail moment with the incubation time. Tail moments were quantified with the computer software 'Comet' using a minimum of 25 cells for each slide (in duplicate).

xenograft tumor models [12,13] and it is currently in clinical trials.

Tafluposide and etoposide share a strong structural homology and the same topoisomerase II target. However, the two compounds act synergistically on acute myeloid leukemia [21]. Tafluposide also shows synergistic activity when it is combined with cisplatin, mitomycin C or doxorubicin [4]. The reason for this is not precisely known, but it is has been attributed to the nucleotide excision repair inhibitory activity of tafluposide [4]. In addition, it is conceivable that tafluposide, which is considerably more hydrophobic than etoposide, exhibits peculiar drug uptake and distribution properties, and perhaps a metabolic pathway distinct from that of etoposide.

Unlike etoposide, tafluposide does not stabilize topoisomerase II–DNA covalent complexes, but acts as a catalytic inhibitor to prevent the enzyme–DNA non-covalent interaction. Nevertheless, the two compounds promote DNA strand breaks in cells. Using V79 Chinese hamster lung fibroblast tumor cells, Barret *et al.* [2] have shown that tafluposide initially induces less DNA strand breaks than etoposide, but the extent of DNA damage increases slowly and linearly with time. Using the same assay we showed here that a similar mechanism is operating in HL-60 human leukemia cells treated with a 10-fold higher concentration of tafluposide (50 μmol/l) versus etoposide (5 μmol/l). In our study, DNA strand breaks were the first events detected, occurring at a much earlier stage with etoposide compared to tafluposide, as

revealed by the Comet assay. It is likely that this initial event exerts a direct influence on the subsequent signals leading to the development of the full apoptosis program. The first mitochondrial modifications are detected a few hours after the detection of DNA damage (4 and 14 h, respectively, for etoposide and tafluposide). For etoposide, the mitochondrial hyperpolarization is the first step of the apoptotic pathway that we have seen, followed by a mitochondrial depolarization (9 and 24 h) and then leading to an increase of the mitochondrial mass (14 and 48 h). The picture is similar for tafluposide in that the order of the events is the same, but with a different time scale. The schematic of the events occurring during the 48-h post-treatment period presented in Fig. 7 helps to understand how the two drugs exert their pro-apoptotic effects. It is tempting to speculate from these diagrams that DNA strand breakage is one (but certainly not a unique) early event that activates the mitochondrial perturbations leading to the apoptotic cell death.

As far as $\Delta\psi_m$ is concerned, the observation of an early hyperpolarization phase followed by a depolarization phase now corresponds to a relatively well-documented process [22–25]. For our part, we have seen this phenomenon with a variety of topoisomerase II inhibitors including etoposide, doxorubicin and the indenoquinolinone derivative TAS-103 [16,18,26]. In contrast, the modification of the mitochondrial mass is a much less well-known effect of anti-tumor drugs. Recently, we have shown that doxorubicin induced an increase of mitochondrial mass in mammary adenocarcinoma MTLn3 cells [16]. Using electronic microscopy, we demonstrated that the drug provoked a marked increase in the number of mitochondria, without a significant sign of swelling, and these proliferating mitochondria remained essentially intact and functional, as judged from their high membrane potential. In HL-60 cells treated with tafluposide or etoposide, the increase of the mitochondrial mass refers to a distinct process because in this case the mitochondrial mass increase occurs after the mitochondrial depolarization. In a recent paper [27], the mitochondrial proliferation induced by etoposide in HL-60 cells has been analyzed by electronic microscopy. The authors showed that, during the late stage of apoptosis, mitochondria were more abundant, but appeared smaller, than those in untreated cells and lacked a proper internal crista structure [27]. This mitochondrial proliferation was accompanied by a significant increase in mtDNA and was inhibited by Bcl-2 overexpression. This process is not specific to HL-60 cells. Etoposide was also shown to induce changes in mitochondrial mass in the hematopoietic stem cell line FDCP-MIX [28]. We hypothesize that mitochondrial proliferation induced by tafluposide occurs in a similar fashion. It is very likely that proliferation of mitochondria is an important step in the cascade of apoptotic events induced by DNA-damaging agents. This event can precede or follow the mitochondrial depolarization and be associated with mitochondrial damage at the ultrastructure level.

**Fig. 7**

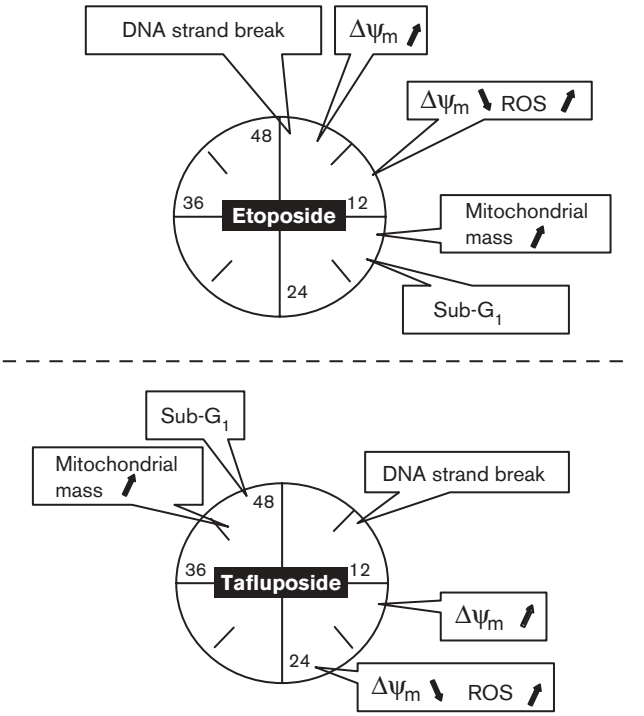


Summary map of biological changes observed in HL-60 cells treated with etoposide and tafluposide. The major events measured in this study and occurring within a period of 48 h after treatment with the indicated drug are indicated, with arrows reflecting (↑) increased or (↓) decreased activity.

The general idea of this paper was (i) to demonstrate the involvement of mitochondria in apoptosis induced by two structurally related topoisomerase II inhibitors acting as DNA strand breakers and (ii) to characterize the kinetics of some of the main events during treatment of HL-60 cells by these DNA-damaging agents. The two objectives have been reached. There is no doubt that mitochondria play a major role in epipodophyllotoxin-induced apoptosis, as least in HL-60 cells. We have evidenced three steps during apoptosis, marked by perturbations of $\Delta\psi_m$ with an initial hyperpolarization phase followed by an irreversible depolarization and a significant increase of the mitochondrial mass, and these events contribute to the appearance of apoptotic cells, but with a different time frame for etoposide versus tafluposide (Fig. 7). We have established a correlation between DNA strand breaks induced by the two drugs and apoptosis progression. The apoptotic development may be delayed and slow if DNA strand breaks appear late, as is the case with tafluposide. In contrast, DNA strand breaks induced extensively and rapidly, as with etoposide, are responsible for the early and fast induction of apoptosis.

## References


1 Perrin D, van Hille B, Barret JM, Kruczynski A, Etievant C, Imbert T, *et al.* F 11782, a novel epipodophylloid non-intercalating dual catalytic inhibitor of topoisomerases I and II with an original mechanism of action. *Biochem Pharmacol* 2000; **59**:807–819.

2 Barret JM, Hill BT, Olive PL. Characterization of DNA-strand breakage induced in V79 cells by F 11782, a catalytic inhibitor of topoisomerases. *Br J Cancer* 2000; **83**:1740–1746.

3 Barret JM, Montaudon D, Etievant C, Perrin D, Kruczynski A, Robert J, *et al.* Detection of DNA-strand breaks in cells treated with F 11782, a catalytic inhibitor of topoisomerases I and II. *Anticancer Res* 2000; **20**:4557–4562.

4 Barret JM, Kruczynski A, Etievant C, Hill BT. Synergistic effects of F 11782, a novel dual inhibitor of topoisomerases I and II, in combination with other anticancer agents. *Cancer Chemother Pharmacol* 2002; **49**:479–486.

5 Barret JM, Cadou M, Hill BT. Inhibition of nucleotide excision repair and sensitization of cells to DNA cross-linking anticancer drugs by F 11782, a novel fluorinated epipodophylloid. *Biochem Pharmacol* 2002; **63**:251–258.

6 Barret JM, Etievant C, Baudouin C, Skov K, Charveron M, Hill BT. F 11782, a novel catalytic inhibitor of topoisomerases I and II, induces atypical, yet cytotoxic DNA double-strand breaks in CHO-K1 cells. *Anticancer Res* 2002; **22**:187–192.

7 Kruczynski A, Barret JM, van Hille B, Chansard N, Astruc J, Menon Y, *et al.* Decreased nucleotide excision repair activity and alterations of topoisomerase IIalpha are associated with the *in vivo* resistance of a P388 leukemia subline to F11782, a novel catalytic inhibitor of topoisomerases I and II. *Clin Cancer Res* 2004; **10**:3156–3168.

8 Jensen LH, Renodon-Corniere A, Nitiss KC, Hill BT, Nitiss JL, Jensen PB, *et al.* A dual mechanism of action of the anticancer agent F 11782 on human topoisomerase II alpha. *Biochem Pharmacol* 2003; **66**:623–631.

9 Kingma PS, Burden DA, Osheroff N. Binding of etoposide to topoisomerase II in the absence of DNA: decreased affinity as a mechanism of drug resistance. *Biochemistry* 1999; **38**:3457–3461.

10 Baldwin EL, Osheroff N. Etoposide, topoisomerase II and cancer. *Curr Med Chem Anticancer Agents* 2005; **5**:363–372.

11 Etievant C, Kruczynski A, Barret JM, Perrin D, van Hille B, Guminski Y, *et al.* F 11782, a dual inhibitor of topoisomerases I and II with an original mechanism of action *in vitro*, and markedly superior *in vivo* antitumour activity, relative to three other dual topoisomerase inhibitors, intoplicin, aclarubicin and TAS-103. *Cancer Chemother Pharmacol* 2000; **46**:101–113.

12 Kruczynski A, Etievant C, Perrin D, Imbert T, Colpaert F, Hill BT. Preclinical antitumour activity of F 11782, a novel dual catalytic inhibitor of topoisomerases. *Br J Cancer* 2000; **83**:1516–1524.

13 Kruczynski A, Ricome C, Waud WR, Hill BT. *In vivo* antitumor activity of F 11782, a non-intercalating dual catalytic inhibitor of topoisomerases I and II, against a panel of human tumor xenografts. *J Exp Ther Oncol* 2002; **2**:219–227.

14 Van Hille B, Etievant C, Barret JM, Kruczynski A, Hill BT. Characterization of the biological and biochemical activities of F 11782 and the bisdioxopiperazines, ICRF-187 and ICRF-193, two types of topoisomerase II catalytic inhibitors with distinctive mechanisms of action. *Anticancer Drugs* 2000; **11**:829–841.

15 Etievant C, Kruczynski A, Barret JM, Perrin D, Hill BT. Apoptotic cell death induction by F 11782 a novel dual catalytic inhibitor of topoisomerases I and II. *Biochem Pharmacol* 2003; **65**:755–763.

16 Kluza J, Marchetti P, Gallego MA, Lancel S, Fournier C, Loyens A, *et al.* Mitochondrial proliferation during apoptosis induced by anticancer agents: effects of doxorubicin and mitoxantrone on cancer and cardiac cells. *Oncogene* 2004; **23**:7018–7030.

17 Salvioli S, Ardizzoni A, Franceschi C, Cossarizza A. JC-1, but not DiOC6(3) or rhodamine 123, is a reliable fluorescent probe to assess delta psi changes in intact cells: implications for studies on mitochondrial functionality during apoptosis. *FEBS Lett* 1997; **411**:77–82.

18 Facompre M, Wattez N, Kluza J, Lansiaux A, Bailly C. Relationship between cell cycle changes and variations of the mitochondrial membrane potential induced by etoposide. *Mol Cell Biol Res Commun* 2000; **4**:37–42.

19 Buckman JF, Hernandez H, Kress GJ, Votyakova TV, Pal S, Reynolds IJ. MitoTracker labeling in primary neuronal and astrocytic cultures: influence of mitochondrial membrane potential and oxidants. *J Neurosci Methods* 2001; **104**:165–176.

20 Guminski Y, Cugnasse S, Fabre V, Monse B, Kruczynski A, Etievant C, *et al.* Synthesis and antitumor activity of a novel epipodophylloid: F 11782, a dual inhibitor of topoisomerases I and II. *Proc Am Ass Cancer Res* 1995; **40**:4510.

21 Sargent JM, Elgie AW, Williamson CJ, Hill BT. *Ex vivo* effects of the dual topoisomerase inhibitor tafluposide (F 11782) on cells isolated from fresh tumor samples taken from patients with cancer. *Anticancer Drugs* 2003; **14**:467–473.

22 Ly JD, Grubb DR, Lawen A. The mitochondrial membrane potential ($\Psi_m$) in apoptosis; an update. *Apoptosis* 2003; **8**:115–128.

23 Scarlett JL, Sheard PW, Hughes G, Ledgerwood EC, Ku HH, Murphy MP. Changes in mitochondrial membrane potential during staurosporine-induced apoptosis in Jurkat cells. *FEBS Lett* 2000; **475**:267–272.

24 Sanchez-Alcazar JA, Ault JG, Khodjakov A, Schneider E. Increased mitochondrial cytochrome c levels and mitochondrial hyperpolarization precede camptothecin-induced apoptosis in Jurkat cells. *Cell Death Differ* 2000; **7**:1090–1100.

25 Pham NA, Hedley DW. Respiratory chain-generated oxidative stress following treatment of leukemic blasts with DNA-damaging agents. *Exp Cell Res* 2001; **264**:345–352.

26 Kluza J, Lansiaux A, Wattez N, Mahieu C, Osheroff N, Bailly C. Apoptotic response of HL-60 human leukemia cells to the antitumor drug TAS-103. *Cancer Res* 2000; **60**:4077–4084.

27 Eliseev RA, Gunter KK, Gunter TE. Bcl-2 prevents abnormal mitochondrial proliferation during etoposide-induced apoptosis. *Exp Cell Res* 2003; **289**:275–281.

28 Reipert S, Berry J, Hughes MF, Hickman JA, Allen TD. Changes of mitochondrial mass in the hemopoietic stem cell line FDCP-mix after treatment with etoposide: a correlative study by multiparameter flow cytometry and confocal and electron microscopy. *Exp Cell Res* 1995; **221**:281–288.